

Stable Optical Rigidity Based on Dissipative Coupling

Albert Nazmiev^{1,*} and Sergey P. Vyatchanin^{1,2}

¹*Faculty of Physics, M.V. Lomonosov Moscow State University, Leninskie Gory, Moscow 119991, Russia*

²*Quantum Technology Centre, Moscow State University, Moscow 119991 Russia*

(Dated: April 21, 2022)

We show that the stable optical rigidity can be obtained in a Fabry-Perot cavity with dissipative optomechanical coupling and with detuned pump, corresponding conditions are formulated. An optical detection of a weak classical mechanical force with usage of this rigidity is analyzed. The sensitivity of small force measurement can be better than the standard quantum limit (SQL).

I. INTRODUCTION

Resonant optomechanics [1] investigates interaction between an optical cavity and a free mass or a mechanical oscillator. The simplest optomechanical interaction is based on the radiation pressure effect in which a force proportional to optical power or number of the optical quanta, circulating in a 1D optical cavity, acts on a test mass so that the size of the optical cavity increases with increase of number of the optical quanta localized in there. Such interaction is usually called as dispersive coupling. Systems having several degrees of freedom allow more complex optomechanical interactions, including radiation pulling (negative radiation pressure) [2, 3], optomechanical interaction proportional to the quadrature of electromagnetic field [4–7] and the interaction depending on the speed and not the coordinate of the mechanical system [8, 9].

Optomechanical interaction is important in precise measurements which use an efficient quantum transduction mechanism between the mechanical and optical degrees of freedom allowing various sensors, like gravitational wave detectors [10–20], torque sensors [21], and magnetometers [22].

Sensitivity of the mechanical coordinate measurement in an optomechanical system usually is restricted by the so-called standard quantum limit (SQL) [23, 24] due to the quantum backaction. The SQL was investigated in various configurations ranging from the macroscopic gravitational wave detectors [7] to the microcavities [25, 26]. Sensitivity of the other types of measurements being derivatives of the coordinate detection is also limited by the SQL. An example of such measurement is detection of a classical force acting on a mechanical degree of freedom of an optomechanical system. However, the SQL of the force measurement is not an unavoidable limit. Several approaches can surpass the SQL, for example, variational measurement [4, 7, 27], optomechanical velocity measurement using dispersive coupling [8, 9], measurements in optomechanical systems with optical rigidity [28, 29]. Quantum speed meter based on dissipative coupling was proposed recently [30].

Among variety of the optomechanical interactions the dissipative coupling takes a special place. The dissipative coupling is characterized by dependence of an optic cavity relaxation on a mechanical coordinate (in case of a Fabry-Perot cavity the mechanical coordinate changes transparency of the input mirror), whereas dispersive coupling is characterized by the dependence of a cavity frequency on the coordinate. The system with dissipative coupling cannot be considered lossless anymore. But the dissipation here does not lead to decoherence or absorption of light, instead, it results in lossless coupling between a continuous optical wave and a mode of an optical cavity. The cavity with dissipative coupling can be used as a perfect transducer between the continuous optical wave and the mechanical degree of freedom, allowing efficient cooling of the mechanical oscillator [21, 31–34], exchange of the quantum states between the optical and mechanical degrees of freedom, mechanical squeezing [35–38], and a combination of cooling and squeezing [39, 40]. A combination of conventional, dispersive, and dissipative coupling adds more complexity to the interaction and leads to the new effects [41, 42].

Dissipative coupling was proposed theoretically [31] and implemented experimentally about ten years ago [21, 32, 33, 43]. It was investigated in different optomechanical systems, including a Fabry-Perot interferometer [21, 32, 33, 43], a Michelson-Sagnac interferometer (MSI) [34, 44, 45], and the ring resonators [41, 42].

In this paper we report on one more important feature of a cavity with dissipative coupling. Such cavity, non-resonantly pumped, introduces a *stable* optical rigidity into the mechanical degree of freedom. Recall that the optical rigidity based on conventional dispersive coupling (in non-resolved side band case) is unstable and can be used only with feedback. We formulate the conditions of stability and show that the stable optical rigidity based on dissipative coupling allows to surpass the SQL.

II. HAMILTONIAN APPROACH

We consider a 1D optomechanical cavity presented on Fig. 1, it's optical mode with eigenfrequency ω_0 is pumped with the detuned light (the pump frequency $\omega_p = \omega_0 + \delta$) — it is generalization of the model in [30]. The optical mode is dissipatively coupled with a mechan-

*Electronic address: nazmiev.ai15@physics.msu.ru

$$F_{lp} = \frac{i\hbar\eta\sqrt{\kappa_0}}{2} \left[A^* a_{in} - A a_{in}^\dagger - A_{in}(a - a_-^\dagger) \right], \quad (2.12)$$

$$a = \frac{\sqrt{\kappa_0} a_{in}}{\frac{\kappa_0}{2} - i(\Omega + \delta)} + \frac{\eta\sqrt{\kappa_0}}{2} \cdot \frac{A_{in} - \sqrt{\kappa_0} A}{\frac{\kappa_0}{2} - i(\Omega + \delta)} \cdot x. \quad (2.13)$$

Here we denote

$$a = a(\Omega), \quad a_-^\dagger = a^\dagger(-\Omega), \quad (2.14a)$$

$$a_{in} = a_{in}(\Omega), \quad a_{in}^\dagger = a_{in}^\dagger(-\Omega). \quad (2.14b)$$

Below we present the light pressure force as a sum

$$F_{lp} = F_{fl} + F_x \quad (2.15)$$

of a fluctuation force F_{fl} and a regular rigidity force F_x proportional to displacement x , which we calculate in next section.

III. OPTICAL RIGIDITY

We substitute Eq. (2.13) into the right part of (2.12) and extract only the term $\sim x$. For the optical rigidity $K = -F_x/x$ one can obtain:

$$K = -m\Omega_0^2 \cdot \frac{\delta \left(\frac{\kappa_0}{2} \left[\frac{3\kappa_0}{2} - 2i\Omega \right] - \delta^2 \right)}{\left[\frac{\kappa_0}{2} \right] \left(\left[\frac{\kappa_0}{2} - i\Omega \right]^2 + \delta^2 \right)}, \quad (3.1)$$

$$\Omega_0^2 = \frac{\hbar\eta^2 A_{in}^2 \left[\frac{\kappa_0}{2} \right]^2}{m \left(\left[\frac{\kappa_0}{2} \right]^2 + \delta^2 \right)} = \frac{\eta^2 \kappa_0 E_0}{4m\omega_p} = \frac{\eta^2 W_{in}}{4m\omega_p} \quad (3.2)$$

Here Ω_0^2 is a recalculated pump (dimension of squared frequency), $E_0 = \hbar\omega_p |A|^2$ is the mean energy stored in the cavity and $W_{in} = \kappa_0 E_0$ is the power of the incident wave.

Recall that in case of dispersive coupling the optical rigidity is always unstable. For example, in case of the detuning on the right slope ($\delta > 0$) of the resonance curve the optical rigidity is positive but the introduced mechanical viscosity is negative, it means instability (in case of the detuning on the left slope the viscosity is positive but the rigidity is negative) [48].

In contrast, the optical rigidity (3.1) is more complicated compared with the rigidity based on dispersive coupling and one can tune both signs of the rigidity and of the viscosity by variation of relation between detuning δ and relaxation rate κ_0 . We can expand (3.1) into the Taylor series over $(-i\Omega)$ keeping only two first terms to demonstrate it:

$$K_m = -m\Omega_0^2 \frac{\delta \left(3 \left[\frac{\kappa_0}{2} \right]^2 - \delta^2 \right)}{\left[\frac{\kappa_0}{2} \right] \left(\left[\frac{\kappa_0}{2} \right]^2 + \delta^2 \right)} - \quad (3.3a)$$

$$- m\Omega_0^2 \frac{4\delta \left(\left[\frac{\kappa_0}{2} \right]^2 - \delta^2 \right)}{\left(\left[\frac{\kappa_0}{2} \right]^2 + \delta^2 \right)^2} (-i\Omega) \quad (3.3b)$$

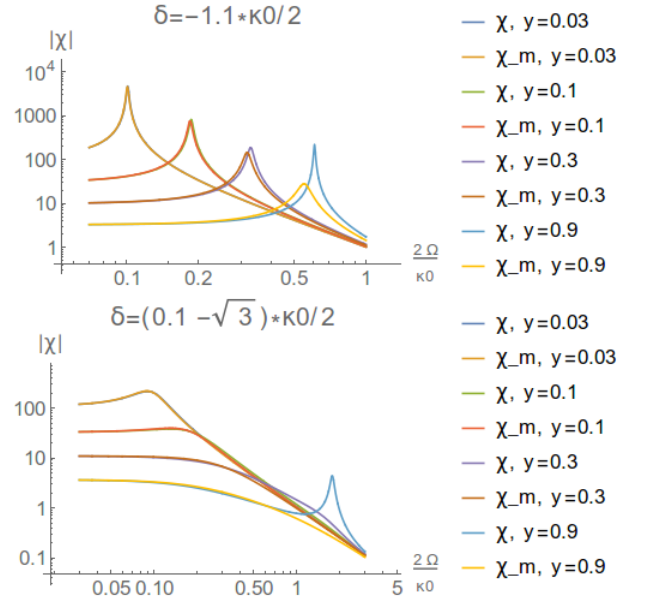


Figure 2: The plots of the susceptibilities $|\chi|$ and their approximations $|\chi_m|$ as function of frequency at detuning $\delta = -1.1 \kappa_0/2$ (upper plot) and $(0.1 - \sqrt{3}) \kappa_0/2$ as function of frequency at the different power parameter y (3.4c).

It is easy to conclude that the rigidity (3.3a) is positive if $\delta < 0$ and $3 \left[\frac{\kappa_0}{2} \right]^2 > \delta^2$, whereas the viscosity (3.3b) is positive if additionally $\left[\frac{\kappa_0}{2} \right]^2 < \delta^2$. So we can formulate the conditions of the stable rigidity:

$$\delta < 0, \quad \frac{\kappa_0}{2} < |\delta| < \sqrt{3} \frac{\kappa_0}{2}. \quad (3.4a)$$

However, conditions (3.4a) are a result of the approximation. For accurate consideration we apply the Routh-Hurwitz criterion [49–52] to investigate stability of the system, described by the susceptibility $\chi = m/(K - m\Omega^2)$, and found that the *accurate* conditions of stability include (3.4a) plus one more condition on the pump

$$0 < \Omega_0^2 < \Omega_{0max}^2, \quad \Omega_{0max}^2 = \frac{\kappa_0}{|\delta|} \left(\delta^2 - \left[\frac{\kappa_0}{2} \right]^2 \right) \quad (3.4b)$$

$$\Omega_0^2 = y\Omega_{0max}^2, \quad 0 < y < 1 \quad (3.4c)$$

Here y is dimensionless power parameter.

Summing up, the rigidity based on dissipative coupling may be positive on *both left and right slopes* of the resonance curve, however, it is stable only on left one, $\delta < 0$.

It is important that we can control characteristics of the *stable* rigidity. We can obtain approximation for eigenfrequency Ω_m , relaxation rate δ_m and quality factor Q_m of a mechanical oscillator created by the optical rigidity using the series (3.3) to demonstrate it:

$$\Omega_m^2 = \frac{\Omega_0^2 |\delta| \left(3 \left[\frac{\kappa_0}{2} \right]^2 - \delta^2 \right)}{\left[\frac{\kappa_0}{2} \right] \left(\left[\frac{\kappa_0}{2} \right]^2 + \delta^2 \right)}, \quad (3.5)$$

$$\delta_m = \frac{2\Omega_0^2 |\delta| \left(\delta^2 - \left[\frac{\kappa_0}{2} \right]^2 \right)}{\left(\left[\frac{\kappa_0}{2} \right]^2 + \delta^2 \right)^2}, \quad (3.6)$$

$$Q_m \equiv \frac{\Omega_m}{2\delta_m} = \frac{\sqrt{3 \left[\frac{\kappa_0}{2} \right]^2 - \delta^2} \left(\left[\frac{\kappa_0}{2} \right]^2 + \delta^2 \right)^{3/2}}{4\Omega_0 \sqrt{|\delta| \left[\frac{\kappa_0}{2} \right]^2} \left(\delta^2 - \left[\frac{\kappa_0}{2} \right]^2 \right)} \quad (3.7)$$

Here we assumed that $\delta < 0$ for stability.

Although this consideration based on the series expansion is convenient, it is valid only for small frequency and small pump. It means that pump parameter Ω_0 must be small. For large pump Ω_0 we have to use the exact susceptibility χ instead of its approximation $\chi_m = m/(K_m - m\Omega^2)$. On Fig. 2 we present the plots of $|\chi|$ and $|\chi_m|$, for the detunings δ , corresponding to the stable rigidity (3.4a) and different y . We see that the approximation (3.3) gives correct results for small power parameter $y \leq 0.3$ whereas for $y > 0.3$ approximation is not valid.

Plots on Fig. 2 also show that choosing detuning δ and power parameter y one can obtain an overdamped mechanical oscillator or an oscillator with high quality factor. So the optical rigidity based on dissipative coupling provides a very promising possibility to create a mechanical system with the characteristics chosen on demand.

Introduction of the stable optical rigidity converts the free mass into the artificially created mechanical oscillator and it is interesting to estimate its noise. Fluctuation force (2.12) impacts on it, its power spectral density S_{Ffl} is equal to

$$S_{Ffl} = 2\hbar m \Omega_0^2 \frac{\left(\left[\frac{\kappa_0}{2} \right]^2 + \delta^2 \right)}{\left[\frac{\kappa_0}{2} \right]^2} \times \left\{ |g_- + j_-|^2 + |g_+ - j_+|^2 \right\}. \quad (3.8)$$

we used the definitions (3.2) and the formula (B5) with the notations in Appendix B. This formula can be rewritten through Ω_m using (3.5).

Due to action of F_{fl} in equilibrium the oscillator possesses mean fluctuation energy $\mathcal{E}_m = m\Omega_m^2 \langle x^2 \rangle$ which is convenient to characterize by mean quantum number n_{eff} :

$$\mathcal{E} = \hbar \Omega_m n_{eff} \quad (3.9)$$

The spectral density S_{Ffl} practically does not depend on spectral frequency Ω and for high quality factor Q_m (3.7) it can be considered as a constant (white noise, not depending on Q_m). Consequently, mean energy \mathcal{E}_m should increase with increase of Q_m . For the particular case our estimate gives

$$n_{eff} \simeq 240, \quad \text{at } \delta = -0.55 \kappa_0, \quad y = 0.01. \quad (3.10a)$$

For these parameters

$$\Omega_m \simeq 0.029 \kappa_0, \quad \kappa_0 \simeq 32.37 \Omega_0, \quad Q_m \simeq 14.5. \quad (3.10b)$$

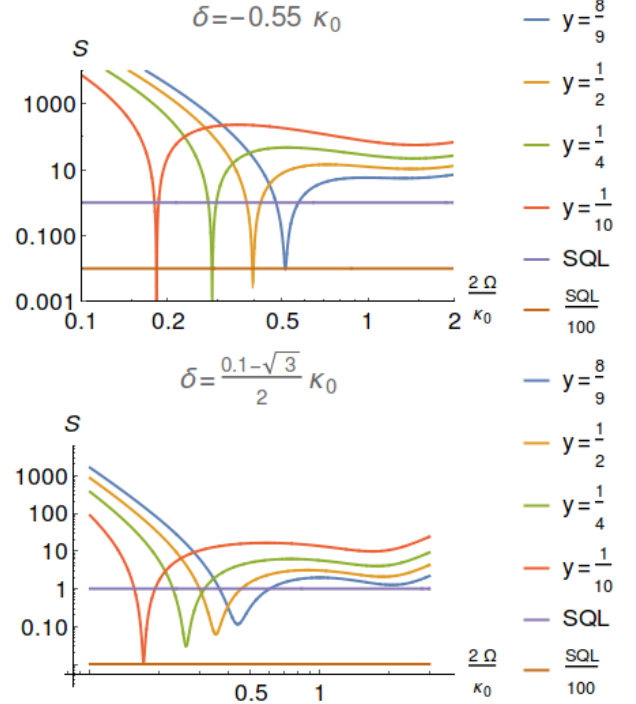


Figure 3: PSD S_f as function of frequency Ω for amplitude detection ($\sin \theta = 0$) with different power parameters y (3.4c). On the top the detuning is $\delta = -5.5 \kappa_0$, on the bottom — $\delta = \frac{0.1 - \sqrt{3}}{2} \kappa_0$.

IV. DETECTION OF SIGNAL FORCE

Using (2.7b, (2.13)) we obtain for the output amplitude in frequency domain:

$$a_{out} = \frac{\frac{\kappa_0}{2} + i[\delta + \Omega]}{\frac{\kappa_0}{2} - i[\delta + \Omega]} a_{in} + \frac{\eta \kappa_0 A_0}{2} \cdot \frac{\frac{\kappa_0}{2} + i\delta}{\frac{\kappa_0}{2} - i\delta} \left(\frac{1}{\frac{\kappa_0}{2} + i\delta} - \frac{1}{\frac{\kappa_0}{2} - i(\delta + \Omega)} \right) \hat{x}, \quad (4.1)$$

We have to substitute the mechanical displacement ξ in frequency domain into (4.1) with account of the rigidity (3.1):

$$x = \frac{F_{fl} + F_s}{-m\Omega^2 Q}, \quad Q = 1 - \frac{K}{m\Omega^2} \quad (4.2)$$

and the fluctuation force F_{fl} (see details in Appendix B).

We assume that the output wave is registered by a homodyne detector. Hence, we have to calculate the quadratures of the output wave. We define the amplitude quadrature e_a and the phase quadrature e_p in the output wave as following:

$$e_a = \frac{1}{\sqrt{2}} \left(\frac{\frac{\kappa_0}{2} - i\delta}{\frac{\kappa_0}{2} + i\delta} a_{out} + \frac{\frac{\kappa_0}{2} + i\delta}{\frac{\kappa_0}{2} - i\delta} a_{out}^\dagger \right), \quad (4.3a)$$

$$e_p = \frac{1}{i\sqrt{2}} \left(\frac{\frac{\kappa_0}{2} - i\delta}{\frac{\kappa_0}{2} + i\delta} a_{out} - \frac{\frac{\kappa_0}{2} + i\delta}{\frac{\kappa_0}{2} - i\delta} a_{out}^\dagger \right). \quad (4.3b)$$

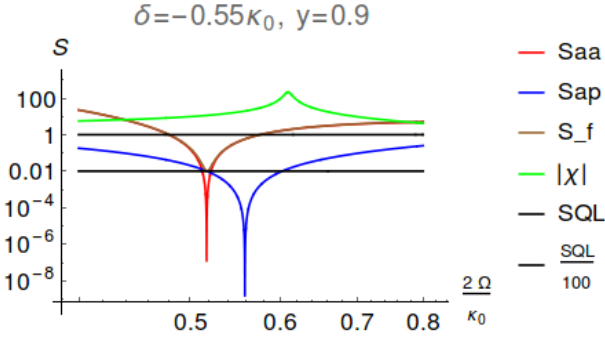


Figure 4: Amplitude detection. Presentation of the contributions by the different terms S_a^A and S_p^A (4.8) into the power spectral density S_f for the particular power parameter $y = 0.9$ and the detuning $\delta = -0.55\kappa_0$. The plot of the susceptibility $|\chi|$ is also presented.

The calculation of the output quadratures as the functions of the input amplitude (a_a) and phase (a_p) quadratures

$$a_a = \frac{a_{in} + a_{in-}^\dagger}{\sqrt{2}}, \quad a_p = \frac{a_{in} - a_{in-}^\dagger}{i\sqrt{2}} \quad (4.4)$$

are presented in Appendix B, the results are:

$$e_a = E_{aa}a_a + E_{ap}a_p + \Phi_a f_s, \quad f_s = \frac{F_s}{\sqrt{2\hbar m \Omega^2}}, \quad (4.5a)$$

$$e_p = E_{pa}a_a + E_{pp}a_p + \Phi_p f_s, \quad (4.5b)$$

Here f_s is a Fourier transform of the signal force normalized to the Standard Quantum Limit (SQL) for the free mass. The expressions for the coefficients in (4.5) are rather cumbersome and we present them using a consequence of notations in Appendix B.

In the homodyne detector we measure a quadrature $e_\theta = e_a \cos \theta + e_p \sin \theta$ in the output wave, where θ is a homodyne angle. Sensitivity is convenient to characterize by the quadrature e_θ recalculated to the SQL:

$$f_\theta = \frac{e_a \cos \theta + e_p \sin \theta}{\Phi_a \cos \theta + \Phi_p \sin \theta} \quad (4.6)$$

with the power spectral density (PSD)

$$S_f(\Omega) = S_a + S_p, \quad (4.7)$$

$$S_a = \frac{|E_{aa} + E_{pa} \tan \theta|^2}{|\Phi_a + \Phi_p \tan \theta|^2}, \quad S_p = \frac{|E_{ap} + E_{pp} \tan \theta|^2}{|\Phi_a + \Phi_p \tan \theta|^2}$$

Below we analyze sensitivity only for the stable rigidity (i.e. the conditions (3.4) are valid).

A. Amplitude detection

Amplitude detection is simpler to realize in experiment as compared with homodyne one. Formally it cor-

responds to $\sin \theta = 0$ in the formulas (4.7):

$$S_f(\Omega) = S_a^A + S_p^A, \quad S_a^A = \frac{|E_{aa}|^2}{|\Phi_a|^2}, \quad S_p^A = \frac{|E_{ap}|^2}{|\Phi_a|^2} \quad (4.8)$$

We obtain that even amplitude detection allows to surpass the SQL (i.e. $S_f < 1$) by more than 100 times. Choosing the pump parameter y one can vary both spectral frequency and range of the SQL surpassing — plots on Fig. 3 demonstrate it.

The top plots on Fig. 3 demonstrate the SQL overcoming by about 1000 times but in the narrow bandwidth. In contrast, the bottom plots demonstrate the more modest SQL overcoming by about 100 times but in the wider bandwidth. Note that the pump power on the top plots is about 10 times lesser than on the bottom ones (with the same pump parameter y).

Analysis shows that the SQL surpassing takes place when the coefficient E_{aa} has minimum due to the compensation of the shot noise term $\sim \beta_+$ and the backaction term $\sim \Omega_0^2$ — see (B7a) in Appendix B. The same compensation takes place for the coefficient E_{ap} in (B7c), but on slightly different spectral frequency Ω .

For demonstration we present on Fig. 4 the contributions of the different terms S_a^A and S_p^A of the spectral density S_f (4.8) for the particular pump parameter $y = 0.9$ and the detuning $\delta = -0.55\kappa_0$. The plot of the susceptibility is also presented (it has different dimension) in order to show that the mentioned compensation takes place on frequencies *different* from frequency Ω_m of mechanical resonance.

B. Homodyne detection

In this case we have the homodyne angle θ as an additional degree of freedom which provides a possibility to control the sensitivity. Indeed, even at the constant pump we can change the PSD by the tuning of the homodyne angle. As shown on Fig. 5 the PSD has a minimum at frequency Ω_{min} and its width $\Delta\Omega$ (where the SQL is surpassed, i.e. $S_f < 1$) can be shifted and changed.

The plots on Fig. 5 demonstrate that frequency Ω_{min} grows with increase of the homodyne angle θ , whereas the bandwidth $\Delta\Omega$ initially decreases until $\Omega_{min} < \Omega_m$ and increases when $\Omega_{min} > \Omega_m$. Note that if $\Omega_{min} \simeq \Omega_m$ we have the most strong minimum of the PSD but in the very narrow bandwidth.

Detailed analysis shows that for the particular plots on top of Fig. 5 the amplitude part S_a makes the main contribution into the PSD (4.7). The minimum of the PSD (practically the minimum of S_a) takes place when the shot noise term $\sim (\beta_+ - \beta_- \tan \theta)$ and the backaction noise term $\sim (E_{aa1} + E_{pa1} \tan \theta)$ compensate each others — for details see formulas (B7) in Appendix B. The plot of the susceptibility is also presented (it has different dimension) in order to show that the mentioned compen-

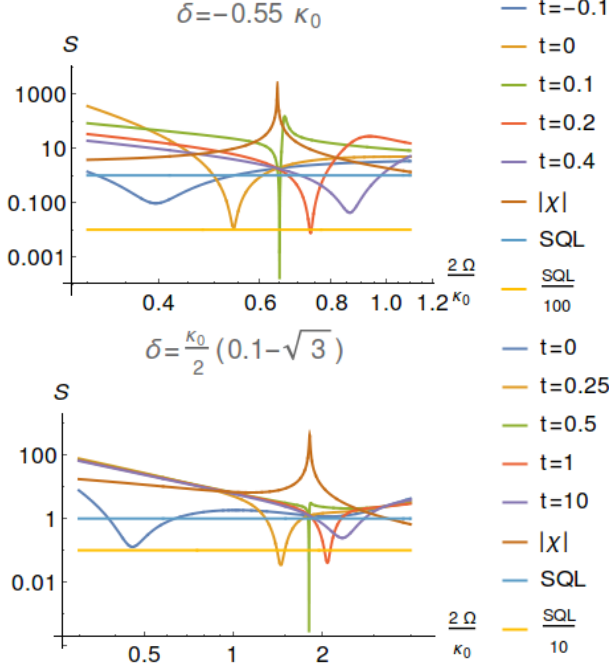


Figure 5: The PSD S_f as a function of frequency Ω for homodyne detection with the constant power parameter $y = 8/9$ (3.4c) at the different homodyne angles $t = \tan \theta$. On the top the detuning is $\delta = -5.5 \kappa_0$, on the bottom — $\delta = \frac{0.1 - \sqrt{3}}{2} \kappa_0$. The plot of the susceptibility $|\chi|$ is also presented.

sation takes place on frequencies *close* to frequency Ω_m of the mechanical resonance.

V. MODEL OF DISSIPATIVE COUPLING BASED ON MICHELSON-SAGNAC INTERFEROMETER

For realization of dissipative coupling without dispersive one we consider a MSI first suggested in [44]. In the Fabry-Perot cavity, shown in Fig. 6, the MSI plays the role of the input generalized mirror (GM). Here we present the generalized model with the non-balanced beam splitter with amplitude transmittance T_{bs} and reflectivity R_{bs} and the partially reflecting mirror M with transmittance T and reflectivity R . We assume that the GM size is smaller than the distance L between the not movable beam splitter and the end mirror so both amplitude transmittance \mathbb{T} and reflectivity \mathbb{R} of the GM depend on position X of movable mirror M with mass m and do not depend on spectral frequency.

We start from the boundary conditions on the beam splitter:

$$A_e = T_{bs} B_c - R_{bs} B_{in}, \quad A_n = R_{bs} B_c + T_{bs} B_{in}, \quad (5.1a)$$

$$B_{out} = T_{bs} B_n - R_{bs} B_e, \quad D_c = T_{bs} B_e + R_{bs} B_n, \quad (5.1b)$$

where B_{in} , B_{out} , B_c , D_c , A_e , A_n , B_e , B_n are the complex amplitudes of the incident and reflected waves on

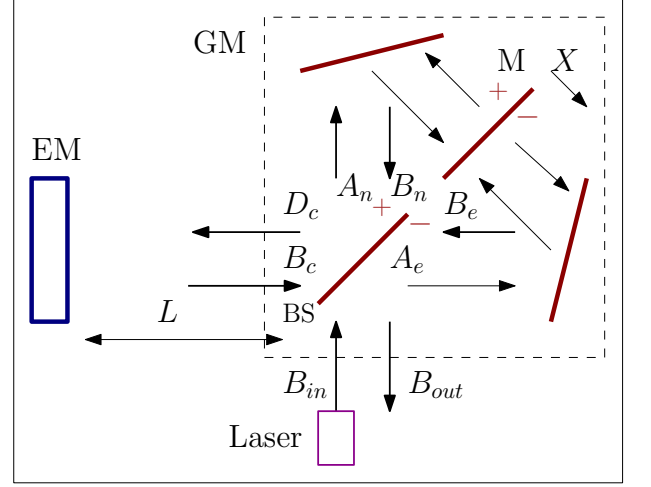


Figure 6: MSI with the input non-balanced beam splitter ($T_{bs} \neq R_{bs}$) and the movable partially reflective mirror M with mass m . It plays the role of the input GM of the cavity pumped by the laser detuned from resonance.

the beam splitter — see the notations on Fig. 6. The boundary conditions on the mirror M give

$$B_e = -R A_e e^{2ik\ell_e} + T A_n e^{ik(\ell_e + \ell_n)}, \quad (5.2a)$$

$$B_n = R A_n e^{2ik\ell_n} + T A_e e^{ik(\ell_e + \ell_n)} \quad (5.2b)$$

where $k = \omega_p/c$ is a wave vector and c is the speed of light, $k\ell_e$ ($k\ell_n$) is the accumulated phase of the light traveling between the beam splitter and the mirror M through the east (north) arm.

We define reflectivity and transmittance of the GM as

$$D_c = \mathbb{T} B_{in} + \mathbb{R}_{\triangleright} B_c, \quad B_{out} = \mathbb{T} B_c + \mathbb{R}_{\triangleleft} B_{in}. \quad (5.3)$$

Using (5.1) and (5.2) one can derive

$$\mathbb{T} = e^{i\phi_+} \{2R R_{bs} T_{bs} \cos \phi_- - T \Delta_{bs}\}, \quad (5.4a)$$

$$\mathbb{R}_{\triangleright} = R e^{i\phi_+} \times \quad (5.4b)$$

$$\times \left\{ \Delta_{bs} \cos \phi_- - i \sin \phi_- + \frac{2T T_{bs} R_{bs}}{R} \right\},$$

$$\mathbb{R}_{\triangleleft} = -R e^{i\phi_+} \times \quad (5.4c)$$

$$\times \left\{ \Delta_{bs} \cos \phi_- + i \sin \phi_- + \frac{2T T_{bs} R_{bs}}{R} \right\},$$

$$\phi_{\pm} = k(\ell_e \pm \ell_n), \quad \Delta_{bs} = R_{bs}^2 - T_{bs}^2 \quad (5.4d)$$

It is obvious that the sum phase ϕ_+ does not depend on the displacement X of the mirror M , but the phase difference ϕ_- does depend. Below we present the displacement $X = x_0 + x$ as a sum of the constant mean value x_0 and the small addition x so that $\phi_- = \phi_0 + 2kx$ and expand reflectivity and transmittance of the GM in a series over x .

One can easily derive that for the realization of pure dissipative coupling (but not combination of dissipative

and dispersive ones) we must have the relative derivatives of \mathbb{T} , $\mathbb{R}_\triangleright$ and \mathbb{R}_\triangleleft over ϕ_- to be real. Calculations give:

$$\frac{\partial_{\phi_-} \mathbb{T}}{\mathbb{T}} = \frac{-2RR_{bs}T_{bs} \sin \phi_-}{2RR_{bs}T_{bs} \cos \phi_- - T\Delta_{bs}}, \quad (5.5a)$$

$$\frac{\partial_{\phi_-} \mathbb{R}_\triangleright}{\mathbb{R}_\triangleright} = \frac{-R\Delta_{bs} \sin \phi_- - iR \cos \phi_-}{R\Delta_{bs} \cos \phi_- - iR \sin \phi_- + 2TT_{bs}R_{bs}}. \quad (5.5b)$$

We see that the relative derivative (5.5a) is real at any combination of the parameters. In order to have the real derivative (5.5b) we have two possibilities:

a) the balanced beam splitter ($\Delta_{bs} = 0$) and the perfectly reflective mirror M ($T = 0$); this case was analyzed in [30, 44];

b) the non-balanced beam splitter and the partially transparent mirror M ($T \neq 0$) — in this case we have to choose $\phi_- = \phi_0$, where ϕ_0 is the solution of equation

$$\cos \phi_0 = \frac{-R\Delta_{bs}}{2TT_{bs}R_{bs}}, \quad (5.5c)$$

$$\mathbb{T}_0 = \mathbb{T}|_{\phi_- = \phi_0} = -e^{i\phi_+} \frac{\Delta_{bs}}{T}, \quad (5.5d)$$

$$|\mathbb{R}_0| = |\mathbb{R}_\triangleright|_{\phi_- = \phi_0} = \frac{\sqrt{(2T_{bs}R_{bs})^2 - R^2}}{T}, \quad (5.5e)$$

$$\left. \frac{\partial_{\phi_-} \mathbb{T}}{\mathbb{T}} \right|_{\phi_- = \phi_0} = \frac{2RT_{bs} \sin \phi_0}{\Delta_{bs}} = \frac{R|\mathbb{R}_0|}{|\mathbb{T}_0|}. \quad (5.5f)$$

The cavity should have high finesse. Hence, for $|\mathbb{T}_0| \ll 1$ one have to have $|\Delta_{bs}| \ll T$. So assuming $e^{i\phi_+} = -1$ we obtain in first order approximation over x

$$\mathbb{T} = \mathbb{T}_0 \left(1 + \frac{R|\mathbb{R}_0|}{|\mathbb{T}_0|} 2kx + \dots \right), \quad (5.6)$$

$$\mathbb{R}_\triangleright = \mathbb{R}_0 \left(1 - \frac{R|\mathbb{T}_0|}{|\mathbb{R}_0|} 2kx + \dots \right). \quad (5.7)$$

We see that for the realization of dissipative coupling with the partially transparent mirror M we should choose the correct angle ϕ_0 (i.e. the constant displacement x_0). It is important that we can choose the parameters of the GM on demand by variation of the beam splitter parameters (R_{bs} , T_{bs}).

The small displacement x of the mirror M from the mean position x_0 provides modulation of the relaxation rate of the Fabry-Perot interferometer:

$$\kappa = \kappa_0(1 + \eta x), \quad \kappa_0 = \frac{|\mathbb{T}|^2}{\tau}, \quad \tau = \frac{2L}{c} \quad (5.8a)$$

$$\eta = 4k \frac{R|\mathbb{R}_0|}{|\mathbb{T}_0|}. \quad (5.8b)$$

It is easy to demonstrate that all equations for this optomechanical system are the same as derived in Sec. II.

It is important that on the example of the considered interferometer as the GM we can demonstrate the peculiar property of a light pressure force in an optomechanical system with dissipative coupling. Indeed, using the

notations on Fig. 6 we can write a ponderomotive force acting on the mirror M:

$$F = 2\hbar k R^2 (|A_n|^2 - |A_e|^2) = \quad (5.9)$$

$$= 4\hbar k R^2 (B_c B_{in}^* + B_c^* B_{in}). \quad (5.10)$$

Here in the last equation we used the input-output relation (5.1) putting $R_{bs} = T_{bs}$. Recall that for dispersive coupling the ponderomotive force is just proportional to the square of the amplitude of the intracavity wave. In contrast, for the optomechanical system with dissipative coupling the force is proportional to the *cross product* of the incident B_{in} and the inside B_c amplitudes as it follows from (5.9). The light pressure force depends on phase difference between B_{in} and \tilde{B}_c , so it can be also called as the *interferometric* pressure. It is precisely this property provides the additional possibilities for the realization of the stable rigidity. We would like to pay attention on resemblance between formulas (5.9) and (2.12), obtained in frame of the Hamiltonian approach.

Note that the realization of the stable optical rigidity was proposed [45] and elegantly demonstrated [34, 53] for a similar scheme with *alone* MSI presented on Fig. 6, without any cavity and without focusing attention on dissipative or dispersive coupling is used. In contrast, in the scheme analyzed in this paper the stable optical rigidity is a property of cavity with dissipative coupling and we formulated the conditions when MSI is a generalized mirror with dissipative coupling (but not a combination of dissipative and dispersive ones).

Conclusion

We analyzed the optical rigidity based on dissipative coupling and formulated the conditions (3.4) of the *stable* optical rigidity. Recall that using dispersive coupling one can get only the *unstable* rigidity [28, 29].

The rigidity based on dissipative coupling may be positive on *the both left and right slopes* of the resonance curve (but stable only on the left one, $\delta < 0$), whereas the positive (unstable) rigidity in case of dispersive coupling takes place on *the right* slope only.

We show that physical reason of stability of the rigidity based on dissipative coupling is interference between the input and intracavity waves, originating the more complicated dependence of the light pressure force as compared with dispersive coupling.

We have shown that dissipative coupling can be realized in the MSI with the partially transparent mirror M — it is the generalization of the previous results [30, 44] for the perfectly reflecting mirror M. It provides the possibility to use a thin membrane [54–56] as the mirror M with extra small mass m for the experimental realization.

For the estimation we assume:

$$m = 10^{-8} \text{ g}, \quad k = \frac{2\pi}{\lambda}, \quad \lambda = 10^{-6} \text{ m}, \quad (5.11a)$$

$$W_{in} = 10^{-4} \text{ W}, \quad R^2 = 0.7, \quad |\mathbb{T}|^2 = 10^{-4} \quad (5.11b)$$

Using (3.2), (3.5) we obtain the estimations of the power parameter Ω_0 and the mechanical eigenfrequency Ω_m :

$$\Omega_0 = \sqrt{\frac{4kW_{in}}{mc|\mathbb{T}|^2}} \simeq 92 \cdot 10^3 \text{ rad/s}, \quad (5.12a)$$

$$\Omega_m \simeq 86 \cdot 10^3 \text{ rad/s}. \quad (5.12b)$$

In the last estimation we put $\delta = -0.55 \kappa_0$.

It means the possibility to create a mechanical nano-oscillator with the eigenfrequency in the range of hundreds kHz from a free mass and the stable optical rigidity. The fluctuation light pressure force is a source of the excitation of the oscillator, we show that in equilibrium the mean quantum number n_{eff} of such oscillator may be about 200. This estimate corresponds to coherent pump, however, for specially tuned squeezed pump mean quantum number n_{eff} can be smaller.

Acknowledgments

Authors acknowledges support from Russian Science Foundation (Grant No. 17-12-01095).

Appendix A: Dissipation Description

In this Appendix we present the detailed description of the Hamiltonian (2.1) and the derivation of the equations (2.2) for the field \hat{a}_c inside cavity and the mechanical coordinate \hat{x} .

We write the Hamiltonians H_T , H_κ in form

$$H_\kappa = -i\hbar \sqrt{\frac{\kappa \Delta\omega}{2\pi}} \sum_{q=1}^{\infty} \left(\hat{a}_c^\dagger \hat{b}_q - \hat{b}_q^\dagger \hat{a}_c \right), \quad (A1)$$

$$H_T = \sum_{q=1}^{\infty} \hbar\omega_q \hat{b}_q^\dagger \hat{b}_q, \quad (A2)$$

Here we present a thermal bath as infinite number of the oscillators with the annihilation and creation operators \hat{b}_q , \hat{b}_q^\dagger , q is integer number, frequencies ω_q of these oscillators are separated by $\Delta\omega = \omega_q - \omega_{q-1}$, we hold in mind that below we put

$$\Delta\omega \rightarrow 0 \quad (A3)$$

The commutators and correlators are

$$[\hat{b}_q, \hat{b}_{q'}^\dagger] = \delta_{qq'}, \quad \langle \hat{b}_q \hat{b}_{q'}^\dagger \rangle = \delta_{qq'}. \quad (A4)$$

(The temperature of the bath is assumed to be zero.) We write down the movement equations:

$$\dot{\hat{a}}_c = \frac{1}{i\hbar} [\hat{a}_c, H] = -i\omega_0 \hat{a}_c - \sqrt{\frac{\kappa \Delta\omega}{2\pi}} \sum_{q=1}^{\infty} \hat{b}_q, \quad (A5a)$$

$$\dot{\hat{b}}_q = -i\omega_q \hat{b}_q + \sqrt{\frac{\kappa \Delta\omega}{2\pi}} \hat{a}_c. \quad (A5b)$$

Introducing the slow amplitudes

$$\hat{a}_c = \hat{a} e^{-i\omega_p t}, \quad \hat{b}_q \Rightarrow \hat{b}_q e^{-i\omega_q t} \quad (A5c)$$

we get

$$\dot{\hat{a}}(t) - i\delta \hat{a} = -\sqrt{\frac{\kappa \Delta\omega}{2\pi}} \sum_{q=1}^{\infty} \hat{b}_q e^{i(\omega_p - \omega_q)t}, \quad (A5d)$$

$$\dot{\hat{b}}_q = \sqrt{\frac{\kappa \Delta\omega}{2\pi}} \hat{a} e^{-i(\omega_p - \omega_q)t}. \quad (A5e)$$

We substitute the formal solution of (A5e) for $\dot{\hat{b}}_q$ into (A5d) using method of successive approximations based on (A3):

$$\hat{b}_q = \hat{b}_q(0) + \sqrt{\frac{\kappa \Delta\omega}{2\pi}} \int_0^t \hat{a}_c(t') e^{-i(\omega_p - \omega_q)t'} dt', \quad (A6a)$$

$$\dot{\hat{a}} - i\delta \hat{a} = -\sum_{q=1}^{\infty} \left(\sqrt{\frac{\kappa \Delta\omega}{2\pi}} \hat{b}_q(0) e^{i(\omega_p - \omega_q)t} - \right. \quad (A6b)$$

$$\left. -\frac{\kappa \Delta\omega}{2\pi} \int_0^t \hat{a}_c(t') e^{i(\omega_p - \omega_q)(t-t')} dt' \right) = \quad (A6c)$$

$$= \sqrt{\kappa} \hat{a}_{in} - \frac{\kappa}{2} \hat{a}. \quad (A6d)$$

Below we present the details of the derivation (A6d).

In the further calculations in the limit (A3) we replace the sum by the integral using the rule

$$\Delta\omega \sum_{q=1}^{\infty} \Rightarrow \int_0^{\infty} d\omega_q. \quad (A7)$$

Using (A4) we calculate the commutator (2.3) for a_{in} defined in (A6b)

$$\hat{a}_{in}(t) \equiv \sqrt{\frac{\Delta\omega}{2\pi}} \sum_{q=1}^{\infty} \hat{b}_q(0) e^{i(\omega_p - \omega_q)t}, \quad (A8a)$$

$$[\hat{a}_{in}(t), \hat{a}_{in}^\dagger(t')] \equiv \frac{\Delta\omega}{2\pi} \sum_{q=1}^{\infty} e^{i(\omega_p - \omega_q)(t-t')} = \quad (A8b)$$

$$= \delta(t - t'), \quad (A8c)$$

Here $\delta(t)$ is the Dirac delta function. By the similar calculation we obtain the correlator (2.4) assuming that the thermostat oscillators are in the main state:

$$\langle \hat{b}_q \hat{b}_{q'}^\dagger \rangle = \delta_{kk'}, \quad \langle \hat{b}_q^\dagger \hat{b}_{q'} \rangle = 0 \quad (A8d)$$

where $\delta_{kk'}$ is the Kronecker delta.

We calculate the term (A6c) using the rule (A7):

$$\int_0^t \hat{a}_c(t') \left[\sum_{q=1}^{\infty} \frac{\kappa \Delta\omega}{2\pi} e^{i(\omega_p - \omega_q)(t-t')} \right] dt' = \quad (A8e)$$

$$= \int_0^t \hat{a}_c(t') \frac{\kappa}{2\pi} \left[\int_0^\infty e^{i(\omega_p - \omega_q)(t-t')} d\omega_q \right] dt' = \quad (\text{A8f})$$

$$= \frac{\kappa}{2\pi} \int_0^t \hat{a}_c(t') 2\pi \delta(t-t') dt' = \frac{\kappa}{2} \hat{a}_c(t). \quad (\text{A8g})$$

From (A1) we get for the mechanical coordinate using the definition (2.2c)

$$\ddot{x} = \frac{i\hbar\eta}{2m} \sqrt{\frac{\kappa_0 \Delta\omega}{2\pi}} \sum_{q=1}^{\infty} (\hat{a}_c^\dagger \hat{b}_q - \hat{b}_q^\dagger \hat{a}_c) + \frac{F_s}{m}. \quad (\text{A9})$$

Using the definition (A8a) we obtain (2.2b).

Appendix B: Calculations of the output quadratures

Here we present the details of calculations for the output quadratures. Here we use the following notations in order to compact the formulas below:

$$\psi = \frac{\kappa_0}{2} - i\delta, \quad \psi^* = \frac{\kappa_0}{2} + i\delta, \quad (\text{B1a})$$

$$\Psi = \frac{\kappa_0}{2} - i\delta - i\Omega, \quad \Psi^* = \frac{\kappa_0}{2} + i\delta + i\Omega, \quad (\text{B1b})$$

$$\Psi_- = \frac{\kappa_0}{2} - i\delta + i\Omega, \quad \Psi_-^* = \frac{\kappa_0}{2} + i\delta - i\Omega, \quad (\text{B1c})$$

For the fluctuation part of the light pressure force F_{fl} in frequency domain we get using (2.12) and the notations (2.14):

$$F_{fl} = \frac{i\hbar A_0 \eta \sqrt{\kappa_0}}{2} \left\{ \frac{a_{in-}^\dagger}{\psi} - \frac{a_{in}}{\psi^*} - \frac{a_{in-}^\dagger}{\Psi_-^*} + \frac{a_{in}}{\Psi} \right\}, \quad (\text{B2})$$

$$g_+ \equiv \frac{\kappa_0}{4} \left(\frac{1}{\psi} + \frac{1}{\psi^*} \right), \quad g_- \equiv \frac{\kappa_0}{4i} \left(\frac{1}{\psi} - \frac{1}{\psi^*} \right), \quad (\text{B3})$$

$$j_+ \equiv \frac{\kappa_0}{4} \left(\frac{1}{\Psi} + \frac{1}{\Psi_-^*} \right), \quad j_- \equiv \frac{\kappa_0}{4i} \left(\frac{1}{\Psi} - \frac{1}{\Psi_-^*} \right). \quad (\text{B4})$$

and express it through the quadratures (4.4) of the input wave

$$F_{fl} = \sqrt{2}\hbar A_0 \eta \{ -a_a(g_- + j_-) + a_p(g_+ - j_+) \} \quad (\text{B5})$$

Substituting it into (4.2) and then into (4.1) using (4.4) we obtain:

$$a_{out} = \frac{\Psi^*}{\Psi} a_{in} + \frac{\eta\kappa_0 A_0}{2} \cdot \frac{\psi^*}{\psi} \left(\frac{1}{\psi^*} - \frac{1}{\Psi} \right) \times \quad (\text{B6})$$

$$\times \frac{\sqrt{2}\hbar A_0 \eta}{-m\Omega^2 Q} \{ -a_a(g_- + j_-) + a_p(g_+ - j_+) \}.$$

Then we substitute it into the definitions (4.3) and after simple but awkward calculations we finally obtain the coefficients in (4.5):

$$E_{aa} = \beta_+ + E_{ag1}, \quad (\text{B7a})$$

$$E_{aa1} = \frac{2\Omega_0^2}{\Omega^2 Q} (g_+ - j_+) (g_- + j_-), \quad (\text{B7b})$$

$$E_{ap} = -\beta_-^* + E_{ap1}, \quad (\text{B7c})$$

$$E_{ap1} = \frac{2\Omega_0^2}{(\Omega^2 Q)} (-g_+ + j_+) (g_+ - j_+), \quad (\text{B7d})$$

$$\Phi_a = \sqrt{\frac{4\Omega_0^2}{\Omega^2}} \left(\frac{-g_+ + j_+}{Q} \right), \quad (\text{B7e})$$

$$E_{pa} = \beta_-^* - E_{pa1}, \quad (\text{B7f})$$

$$E_{pa1} = \frac{2\Omega_0^2}{\Omega^2 Q} (g_- + j_-) (g_- + j_-), \quad (\text{B7g})$$

$$E_{pp} = \beta_+ + E_{pp1}, \quad (\text{B7h})$$

$$E_{pp1} = \frac{2\Omega_0^2}{\Omega^2 Q} (g_- + j_-) (g_+ - j_+), \quad (\text{B7i})$$

$$\Phi_p = \sqrt{\frac{4\Omega_0^2}{\Omega^2}} \left(\frac{g_- + j_-}{Q} \right). \quad (\text{B7j})$$

where

$$\beta_+ = \frac{1}{2} \left(\frac{\psi\Psi^*}{\psi^*\Psi} + \frac{\psi^*\Psi_-}{\psi\Psi_-^*} \right), \quad (\text{B8a})$$

$$\beta_- = \frac{1}{2i} \left(\frac{\psi\Psi^*}{\psi^*\Psi} - \frac{\psi^*\Psi_-}{\psi\Psi_-^*} \right) \quad (\text{B8b})$$

and Ω_0^2 is the normalized pump (3.2).

-
- [1] M. Aspelmeyer, T. Kippenber, and F. Marquardt, Reviews of Modern Physics **86**, 1391–1452 (2014).
 - [2] M. L. Povinelli, M. Lončar, M. Ibanescu, E. J. Smythe, S. G. Johnson, F. Capasso, and J. D. Joannopoulos, Opt. Lett. **30**, 3042–3044 (2005), URL <http://ol.osa.org/abstract.cfm?URI=ol-30-22-3042>.
 - [3] A. V. Maslov, V. N. Astratov, and M. I. Bakunov, Phys. Rev. A **87**, 053848 (2013), URL <http://link.aps.org/doi/10.1103/PhysRevA.87.053848>.
 - [4] S.P. Vyatchanin and A.B. Matsko, Sov.Phys – JETP **77**,

- 218–221 (1993).
- [5] S.P. Vyatchanin and A.B. Matsko, Sov. Phys. – JETP **82**, 107 (1996).
- [6] A.B. Matsko and S.P. Vyatchanin, Applied Physics B **64**, 167–171 (1997), ISSN 1432-0649, URL <http://dx.doi.org/10.1007/s003400050161>.
- [7] H.J. Kimble, Y. Levin, A.B. Matsko, K.S. Thorne, and S.P. Vyatchanin, Phys. Rev. D **65**, 022002 (2001), arXiv:gr-qc/0008026v2.
- [8] V.B. Braginsky and F.Ya. Khalili, Physics Letters A

- 147**, 251–256 (1990).
- [9] V.B. Braginsky, M.L. Gorodetsky, F.Y. Khalili, and K.S. Thorne, *Physical Review D* **61**, 044002 (2000).
 - [10] LVC-Collaboration, arXiv **1304.0670** (2013).
 - [11] Y. Aso et al., *Phys. Rev. D* **88**, 043007 (2013).
 - [12] K. Dooley, T. Akutsu, S. Dwyer, and P. Puppo, arXiv **1411.6068** (2014).
 - [13] C. Affeld, K. Danzmann, K. Dooley, H. Grote, M. Hewitson, S. Hild, J. Hough, J. Leong, H. Luck, and M. Prijatelj, *Classical and Quantum Gravity* **32**, 224002 (2104).
 - [14] J. Aasi et al (LIGO Scientific Collaboration) et al., *Classical and Quantum Gravity* **32**, 074001 (2015).
 - [15] F. Acernese et al, (Virgo Collaboration), *Classical and Quantum Gravity* **32**, 024001 (2015).
 - [16] B.P. Abbott et al, (LIGO Scientific Collaboration, Virgo Collaboration and KAGRA Collaboration), *Living Reviews in Relativity* **21**, 3 (2018).
 - [17] B. P. Abbott et al, (LIGO Scientific Collaboration and Virgo Collaboration), *Phys. Rev. Lett.* **116**, 241103 (2016).
 - [18] B.P. Abbott et al, (LIGO Scientific Collaboration and Virgo Collaboration), *Phys. Rev. Lett.* **119**, 161101 (2017).
 - [19] B.P. Abbott et al, (LIGO Scientific Collaboration and Virgo Collaboration), *Phys. Rev. Lett.* **119**, 141101 (2017).
 - [20] F. Acernese et al (Virgo Collaboration), arXiv **1807.03275** (2018).
 - [21] M. Wu, A.C. Hryciw, C. Healey, D.P. Lake, H. Jayakumar, M.R. Freeman, J.P. Davis, and P.E. Barclay, *Physical Review X* **4**, 021052 (2014).
 - [22] S. Forstner and S. Prams and J. Knittel and E.D. van Ooijen and J.D. Swaim and G.I. Harris and A. Szorkovszky and W.P. Bowen and H. Rubinsztein-Dunlop, *Physical Review Letters* **108**, 120801 (2012).
 - [23] V.B. Braginsky, *Sov. Phys. JETP* **26**, 831–834 (1968).
 - [24] V.B. Braginsky and F.Ya. Khalili, *Quantum Measurement* (Cambridge University Press, Cambridge, 1992).
 - [25] T. Kippenberg and K. Vahala, *Science* **321**, 1172–1176 (2008).
 - [26] J.M. Dobrindt and T.J. Kippenberg, *Physical Review Letters* **104**, 033901 (2010).
 - [27] S. Vyatchanin and E. Zubova, *Physics Letters A* **201**, 269–274 (1995).
 - [28] V.B. Braginsky and F.Ya. Khalili, *Phys. Lett. A* **257**, 241 (1999).
 - [29] F.Ya. Khalili, *Physics Letters A* **288**, 251–256 (2001), arXiv:gr-qc/0107084.
 - [30] S.P. Vyatchanin and A.B. Matsko, *Physical Review A* **93**, 063817 (2016).
 - [31] F. Elste and S.M. Girvin and A.A. Clerk, *Physical Review Letters* **102**, 207209 (2009).
 - [32] M. Li and W.H.P. Pernice and H.X. Tang, *Physical Review Letters* **103**, 223901 (2009).
 - [33] A. Hryciw, M. Wu, B. Khanaliloo, and P. Barclay, *Optica* **2**, 491 (2015).
 - [34] A. Sawadsky, H. Kaufer, R. Nia, S. Tarabrin, F. Khalili, K. Hammerer, and R. Schnabel, *Physical Review Letters* **114**, 043601 (2015).
 - [35] A. Kronwald and F. Marquardt and A.A. Clerk, *Physical Review A* **88**, 063833 (2013).
 - [36] H. Tan, G. Li, and P. Meystre, *Physical Review A* **87**, 033829 (2013).
 - [37] J. Zhu, H. Huang, and G. Li, *Journal of Applied Physics* **115**, 033102 (2014).
 - [38] K. Qu and G.S. Agarwal, *Physical Review A* **91**, 063815 (2015).
 - [39] W.G. Gu and G.X. Li and Y.P. Yang, *Physical Review A* **88**, 013835 (2013).
 - [40] W. Gu and G. Li, *Optics Express* **21**, 20423 (2013).
 - [41] S. Huang and G.S. Agarwal, *Physical Review A* **81**, 053810 (2010).
 - [42] S. Huang and G.S. Agarwal, *Physical Review A* **82**, 033811 (2010).
 - [43] T. Weiss, C. Bruder, and A. Nunnenkamp, *New Journal of Physics* **15**, 045017 (2013).
 - [44] A. Xuereb, R. Schnabel, and K. Hammerer, *Physical Review Letters* **107**, 213604 (2011).
 - [45] S. Tarabrin, H. Kaufer, F. Khalili, R. Schnabel, and K. Hammerer, *Physical Review A* **88**, 023809 (2013).
 - [46] A.A. Clerk and M.H. Devoret and S.M. Girvin and F. Marquardt and R.J. Schoelkopf, *Reviews of Modern Physics* **82**, 1155 (2010), arXiv:08104729.
 - [47] F. Marquardt and S. Girvin, *Physics* **2**, 40 (2009).
 - [48] V.B. Braginsky, I.I. Minakova, *Vestnik Moskovskogo Universiteta, Seriya 3* p. 69 (1964), in *Russian*.
 - [49] E. Routh, *A Treatise on the Stability of a Given State of Motion: Particularly Steady Motion* (Macmillan, 1877).
 - [50] A. Hurwitz, *Math. Ann.* **46**, 273–284 (1895).
 - [51] M. Rabinovich and D. Trubetskov, *Introduction into Theory of Oscillations and Waves (in Russian)* (Nauka, Moscow, 1984).
 - [52] M. Gopal, *Control Systems: Principles and Design* (Tata McGraw-Hill Education, 2002), 2nd ed.
 - [53] J. Cripe, B. Danz, B. Lane, M. Lorio, J. Falcone, G. Cole, and T. Corbitt, *Optics Letters* **43**, 2193 (2018).
 - [54] O. Arcizet, P.-F. Cohadon, T. Briant, M. Pinard, A. Heidmann, J.-M. Mackowski, C. Michel, L. Pinard, O. Francais, and L. Rousseau, *Physical Review Letters* **97**, 133601 (2006).
 - [55] B. M. Zwickl, W. E. Shanks, A. M. Jayich, C. Yang, A. C. B. Jayich, J. D. Thompson, and J. G. E. Harris, *Applied Physics Letters A* **92**, 103125 (2008).
 - [56] K. Borkje, A. Nunnenkamp, B. Zwickl, C. Yang, J. Harris, and S. Girvin, *Physical Review A* **82**, 013818 (2010).